Electrochimica Acta 222 (2016) 1700–1708

Contents lists available at ScienceDirect

Electrochimica Acta

journal homepage: www.elsevier.com/locate/electacta

Electrochemical study of azide bridged heterobimetallic films of porphyrins: Application as an impedimetric sensor

Romina Carballo[1], Ana L. Rinaldi, Irene N. Rezzano*,[1]

Universidad de Buenos Aires, Consejo Nacional de Investigaciones Científicas y Técnicas, Instituto de Química y Fisicoquímica Biológicas (IQUIFIB), Facultad de Farmacia y Bioquímica, Buenos Aires, Argentina

ARTICLE INFO

Article history:
Received 27 September 2016
Received in revised form 22 November 2016
Accepted 27 November 2016
Available online 28 November 2016

Keywords:
impedimetric sensor
metalloporporphyrins
films
linked azide

ABSTRACT

In this study, heterobimetallic films of metalloporphyrins, polyCo(II)PP and polyNi(II)PP, linked with azide (polyCoN_3NiPP) were immobilized on a glassy carbon electrode. The intense FTIR absorption band at 2056 cm^{-1}, corresponding to the ν_{asy} (N_3) of the bridged azide, indicates a μ2-coordination mode of polyCoN_3NiPP. The electrochemical characterization of the films clearly shows that the order of deposition significantly affects the charge transfer process, correlated to the organized polymeric structure. The linked azide anion shows a reversible wave exclusively in the configuration polyNi(II)PP deposited over a film of polyCo(II)PP. The Nyquist plots of this electrode, using $Fe(CN)_6{}^{3-}$/$Fe(CN)_6{}^{4-}$ as redox probe, demonstrated a lower R_{ct} and higher K_{app} than other configurations. This electrode was applied as an impedimetric sensor for sulfite anion.

1. Introduction

In the last years, functional materials with a diversity of chemical structures and relevant physicochemical properties have played a significant role in several technological areas [1]. The correlation between structure or microstructure and functionality is usually achieved by combining building blocks with unique optical, electronic or redox characteristics and metal binding sites for orthogonal coordination.

Research on molecular electronics focuses on the structure of the building blocks because the electron currents through molecules connected to electrodes are ruled by the gap between the highest occupied molecular orbital (HOMO) and lowest unoccupied molecular orbital (LUMO), the spin, and the vibrational modes of the molecules [2].

In the particular case of metal organic complexes, there is a continuing interest in the multinuclear 3d molecular metal clusters (Mn(III), Fe(III), Co(II) and Ni(II)) because they usually show fascinating structures and attractive electronic and magnetic properties [3].

The intense research in the field has demonstrated that the formation of mixed-valence states favors the increase of the electrical conductivity. In fact, the strength of electronic interaction between the oxidized and reduced sites ranges from zero (Class I) to weak or moderate (localized valence, Class II) or to very strong electronic coupling (delocalized valence, Class III) [4].

Metalloporphyrins are aromatic structures with versatile redox properties, highly dependent of the central metal and the type of axial ligand incorporated. The π system of the porphyrin is an efficient platform for electron transfer that has been described as a Class III, with ferrocenyl substituents [5].

We observed a synergic effect between the redox centers in heterobimetallic films of porphyrins in comparison with their monometallic counterparts [6–8]. This behavior was attributed to the overlapping of the charge-transfer transitions of the two porphyrin complexes and the formation of a mixed-valence heterobinuclear complex, that only occurs with the combinations Fe/Cu and Fe/Ni. Similar results have been reported for another type of ligands where the orientation of the two metal centers defines the functional behavior [9].

Another relevant example of bimetallic center, with porphyrins, correspond to the metallo-enzyme sulfite oxidase that utilizes a molybdopterin cofactor and a heme group. Current mechanistic proposals involve the transfer of an oxygen atom from the metallic center to yield sulfate [10], which is highly dependent of the proximity of the redox sites [11]. This process is closely associated

* Corresponding author.
E-mail addresses: irezzano@ffyb.uba.ar, irezzano@yahoo.com.ar (I.N. Rezzano).
[1] CONICET permanent staff.

http://dx.doi.org/10.1016/j.electacta.2016.11.161
0013-4686/

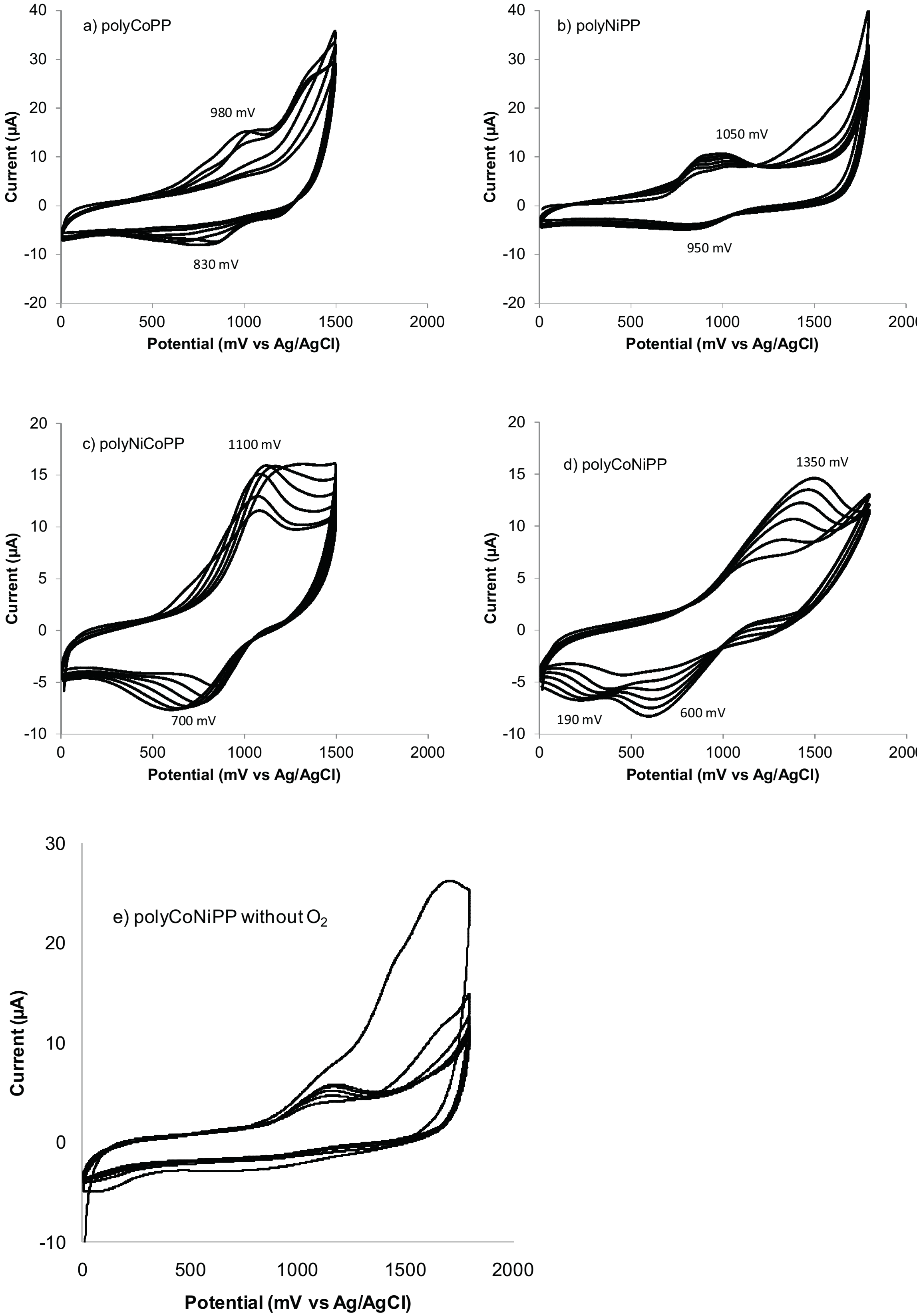

Fig. 1. Cyclic voltammograms obtained during electropolymerization onto glassy carbon electrodes of: (a) polyCoPP; (b) polyNiPP; (c) polyCoPP over polyNiPP (polyNiCoPP); (d) polyNiPP over polyCoPP (polyCoNiPP); (e) polyNiPP over polyCoPP without oxygen (polyCoNiPP). Linear sweep 0.00 to +1.50 V (vs Ag/AgCl) and 0.00 to +1.80 V (vs Ag/AgCl) by CoPP and NiPP, respectively. Scan rate 0.05 V s^{-1}, six cycles.

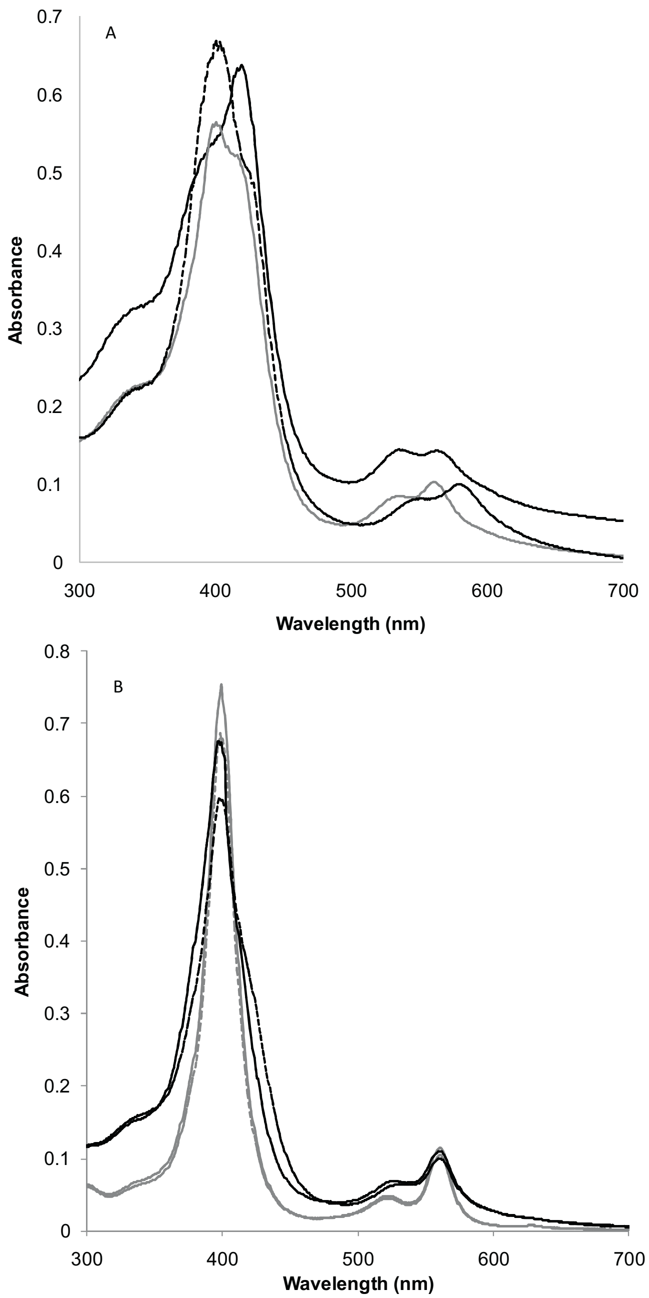

Fig. 2. Uv-Vis spectra of: A) (black dotted line) polyCoPP; (black line) polyCoPP with azide added; (gray line) polyCoPP azide after NiPP added; B) (gray line) polyNiPP; (gray dotted line) polyNiPP with azide; (black line) polyCoNiPP and (black dotted line) polyCoNiPP with azide added.

to the intramolecular electron transfer in mixed-valence complexes.

The azide anion is an excellent bridging ligand for transition metal ions, which shows some binding modes when incorporated into an array of 1D, 2D, and 3D coordination polymers. When it is introduced in rigid aromatic structures, the $\pi-\pi$ interactions between an azide and the aromatic rings establish new resonant forms that favor the electron transfer [12,13]. The N_3^- anion can be incorporated as an axial ligand of oxygenated complexes of Co as a bridge between two metal ions, adopting a μ2-coordination mode, or through one N atom as a monodentate terminal ligand. Recently, a new tetranuclear mixed-valence cobalt complex has been synthesized containing two Co(II) cations and two Co(III) cations which are bridged by two organic ligands and two μ2-N_3 anions to form a tetranuclear $[Co_4N_4O_4]$ cluster [14].

Here, we study the incorporation of N_3^- to polymeric metalloporphyrins preparation, with the aim of increasing the electronic properties of the films. The heterobimetallic structures containing polyCo(II)PP and polyNi(II)PP, linked with the azide anion, are characterized by spectroscopic and electrochemical methods. The resulting modified electrode is applied to evaluate the charge transfer in sulfite oxidation.

2. Experimental

2.1. Reagents

Metalloprotoporphyrin complexes were prepared according to standard procedure [15]. Tetrabutylammonium perchlorate (TBAP) was obtained by precipitation of a saturated solution of the tetrabutylammonium hydroxide (Sigma-Aldrich) with perchloric acid and twice recrystallized from ethanol and dried in under vacuum. $K_3Fe(CN)_6$ (99%), NaN_3 (99%), KBr (99%), KCl (99%)and Na_2SO_3 (98%) were of analytical grade (Sigma-Aldrich). Water was deionized and filtered using a Millipore water purification system (18 MΩ).

2.2. Apparatus

Cyclic voltammetry (CV) and amperometric detection were performed with a purpose built potentiostat (TEQ-Argentina), with a digital signal generator for implementation of different electrochemical techniques. Electrochemical impedance spectra were recorded using a potentiostat TEQ4-Z (TEQ-Argentina) and a frequency response analyzer. Data analysis was performed with the program ZView® (Scribner Associates, USA).

A glassy carbon working electrode (0.25 cm^2 area), an Ag/AgCl KCl 3 M reference electrode (BAS) and a platinum wire auxiliary electrode were used for voltammetric and electrochemical impedance experiments. Impedance measurements were performed with a purpose built Teflon cell.

FTIR spectra were recorded on a Nicolet 360 spectrometer using KBr pellets. All spectra were collected at 4 cm^{-1} spectral resolution using 64 scans.

An HP8452 diode array spectrophotometer, a 1 cm^2 geometric area indium tin oxide on glass substrate (ITO) working electrode (Goodfellow) and a quartz crystal cell were used to obtain the UV spectra.

2.3. Electrode preparation

The glassy carbon electrode was polished with 0.3 and 0.05 μm diameter alumina particles and finally rinsed with deionized water.

The electropolymerization of metalloprotoporphyrins (1 mM) onto the glassy carbon electrode (GCE) was carried out in 0.1 M TBAP/CH_2Cl_2 by potential sweep between 0.00 and +1.50 V (vs. Ag/AgCl) by CoPP at 0.05 V s^{-1} six cycles, and between 0.00 to +1.8 V (vs. Ag/AgCl) by NiPP at 0.05 V s^{-1} six cycles [7]. Bimetallic porphyrinic modified electrodes were prepared by polymerizing CoPP and then NiPP or NiPP and then CoPP under those same conditions for polyCoNiPP or polyNiCoPP, respectively.

To obtain the polyMePPN_3 (Me = Co or Ni), mono and bimetallic structures, polyporphyrinic modified glassy carbon electrodes were immersed and left in contact for at least 4 hours in 10 mM sodium azide aqueous solution.

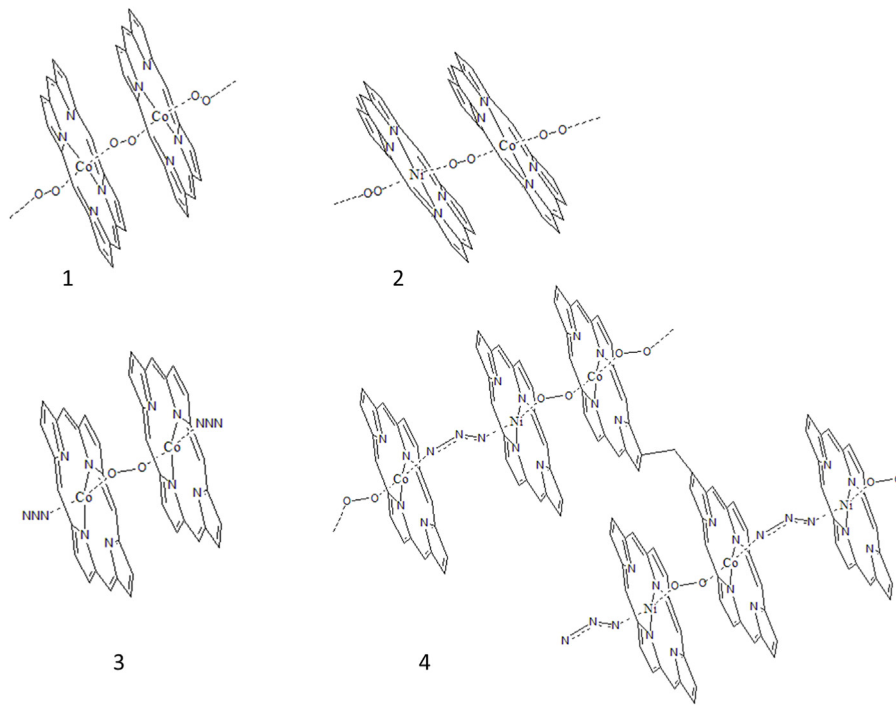

Scheme 1. Possible coordination modes for ligands.

2.4. Electrochemical impedance spectroscopy (EIS)

All the electrochemical experiments were performed in the presence of oxygen. The frequency range was 100 kHz to 0.1 Hz, and the amplitude of oscillation was set to 10 mV_{RMS}. The electrochemical experiments in the presence of 5 mM $K_3Fe(CN)_6$ were carried out in 0.1 M KCl. The working potential was set to +0.250 V (vs. Ag/AgCl) for EIS measurements.

To evaluate the applicability of the $polyCoN_3NiPP/GCE$ as a sensor for sulfite, the electrochemical experiments were carried out in 0.05 M KH_2PO_4/K_2HPO_4 buffer solution (pH 7.0). In EIS measurements, the analytical performance was evaluated in the range of 0–3.4 mM and the working potentials were +0.7 V and +1.1 V for $polyCoN_3NiPP/GCE$ and bare glassy carbon electrode, respectively.

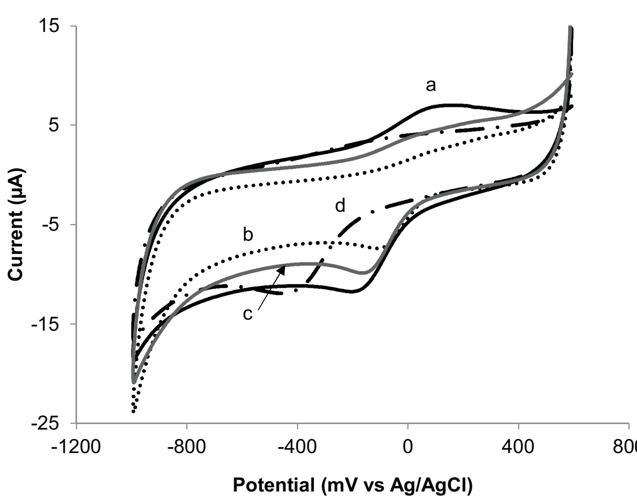

Fig. 3. Cyclic voltammetric response of (a) polyCoNiPP; (b) polyCoPP; (c) polyNiCoPP; (d) polyNiPP in 0.1 M KCl with 5 mM sodium azide added. Scan rate 0.05 V s^{-1}.

2.5. Real samples

All analytical studies in real samples were performed using EIS at +0.7 V with $polyCoN_3NiPP/GCE$. The measurements were conducted by adding 5 mL of sample to 500 µL of 0.5 M KH_2PO_4/K_2HPO_4 buffer solution (pH 7.0), as the supporting electrolyte. Standard addition method was employed for wine sample analysis. These experiments were performed with sulfite-free samples and samples with addition of sodium sulfite (0.2, 0.5, 1 and 2 mM of SO_3Na_2 added). A homemade white wine freshly prepared was used as sulfite-free wine samples.

3. Results and discussion

3.1. Characterization of the bimetallic films

The electrodes were modified by the sequential deposition of the polymers of metalloporphyrins [7]. Fig. 1a and b show voltammograms obtained during the electropolymerization of the two metallic complexes of porphyrin, corresponding to Co(II) Protoporphyrin (polyCoPP) and Ni(II) Protoporphyrin (polyNiPP), respectively. Meanwhile, Fig. 1c shows the electropolymerization process of CoPP over a thin layer of polyNiPP (polyNiCoPP) and reversely, Fig. 1d the deposition of NiPP over a film of polyCoPP (polyCoNiPP). The increase of anodic and cathodic peak currents on successive scans can be observed in all the voltammograms, indicating that the electrodeposition takes place at a positive potential where the radical cation is formed [16]. All the experiments were carried out with and without oxygen, but only the bimetallic structure polyCoNiPP (Fig. 1d and e) is depicted in both conditions. Relevant data is the cathodic peak at 190 mV

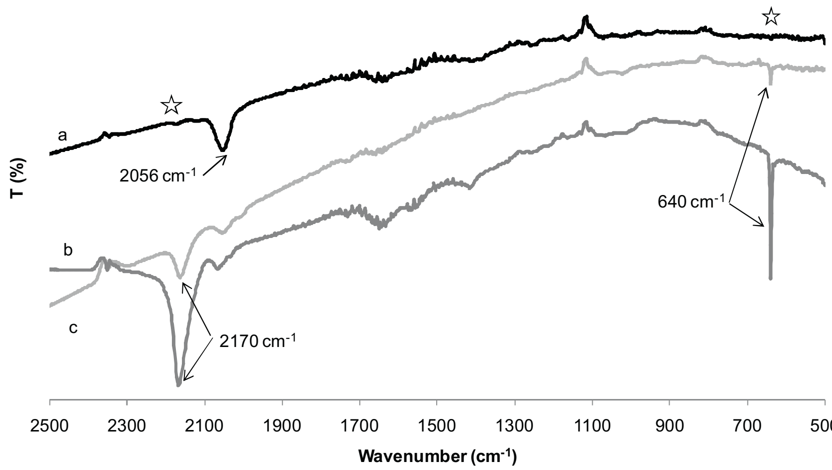

Fig. 4. FTIR spectra of (a) polyCoNiPP (b) polyNiPP and (c) polyCoPP after all were treated with sodium azide. Stars indicate the disappeared peaks.

(Fig. 1d), which is observed exclusively in the presence of oxygen and could correspond to the reduction of a bimetallic peroxo intermediate [17].

The UV–vis spectra reinforce that idea, Fig. 2 compares the absorption spectra of the mono and bimetallic polymers either with or without a previous incorporation of azide N_3^-. The peaks at 406 and 546 nm in polyCoPP are consistent with the presence of polyCoPPO_2^-, which is expected from the tendency of Co(III) complex to accommodate oxygen as the fifth ligand in aerobic conditions [18,19] (**1** in Scheme 1). These peaks are shifted to 421 and 536 nm in the polyCoPP pretreated with azide, indicating a ligand exchange process in formation of the mononuclear Co(III) species with a terminal azide ion, polyCoPPN_3^- (**3** in Scheme 1). In turn, the UV-visible spectrum of polyCoN_3NiPP is very similar to that of NiPP in solution (~400 nm and 560 nm) with an additional small shoulder at 420 nm (Fig. 2B).The polyNiPP in the presence of azide does not show any change. To further investigate this result, we made another experiment that consists in adding NiPP to the polyCoPPN_3^-. Interestingly, the peak at 421 nm decreases with the simultaneous growth of the band at 402 nm until a 1:1 stoichiometric ratio of metals is reached in polyCoN_3NiPP (Fig. 2A). At this point, the species polyCoN_3NiPP (**4** Scheme 1) is reached.

The ΔEps of the different modified electrodes are 100, 150, 400 and 750 mV corresponding to NiPP, CoPP, CoPP over NiPP and NiPP over CoPP respectively. These values suggest a high production of mixed-valence states, especially in the polyNiPP over polyCoPP assembly (polyCoNiPP), taking into account that the increase of ΔEp is consistent with the higher strength of the interaction between the redox sites [4]. This effect is maximun in the polyCoN_3NiPP film, where a reversible anodic wave is obtained (Fig. 3a) in the presence of oxygen. The Co(III) and Ni(II) complexes can be further oxidized to high valence intermediate species under these experimental conditions. The wave desappears after argon bubbling.

Undoubtedly, the initial deposit of a hexacoordinated oxo Co(III) is required to establish a preferred geometry of the metal centers, which results in the unique electrochemical properties of the polyCoNiPP including the efficient incorporation of N_3^- as a linker between the metal centers.

Fig. 4 depicts the infrared spectra of the different polymers mono NiPP, CoPP and bimetallic Co-NiPP in the presence of azide. The structure of the azido-bridged binuclear complexes was studied following the asymmetric stretching mode of the azide ion at ~2000 cm^{-1}. The intense absorption band at 2056 cm^{-1} is attributed to the ν_{asy} (N_3) of the bridged azide between the bimetallic structure polyCoNiPP (polyCoN_3NiPP) in agreement with the previous report of Collman's group for mixed valence $Fe^{3+}N_3^-Cu^{2+}$complexes [17]. Additionally, the typical vibrational binding scissors band of the free azide in solution at 640 cm^{-1} disappears in the FTIR spectra of the polyCoN_3NiPP, corroborating the N_3^- bridged structure.

3.2. Electrochemical response of azide bridged bimetallic film (polyCoN_3NiPP)

Electrochemical impedance spectroscopy (EIS) can be used as an effective technique to evaluate the complex electrochemical behavior of the modified electrodes. For this purpose, the electrical conduction of different mono and bimetallic modified electrodes

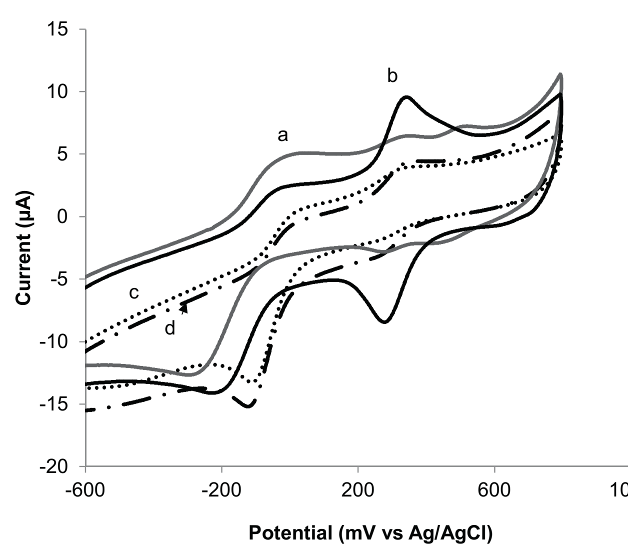

Fig. 5. Cyclic voltammetric response in 0.1 M KCl containing 5 mM $Fe(CN)_6^{3-/4-}$ before (a and c) and after (b and d) treatment with azide for: (a) and (b) polyCoNiPP; (c) and (d) polyCoPP. Scan rate 0.05 V s^{-1}.

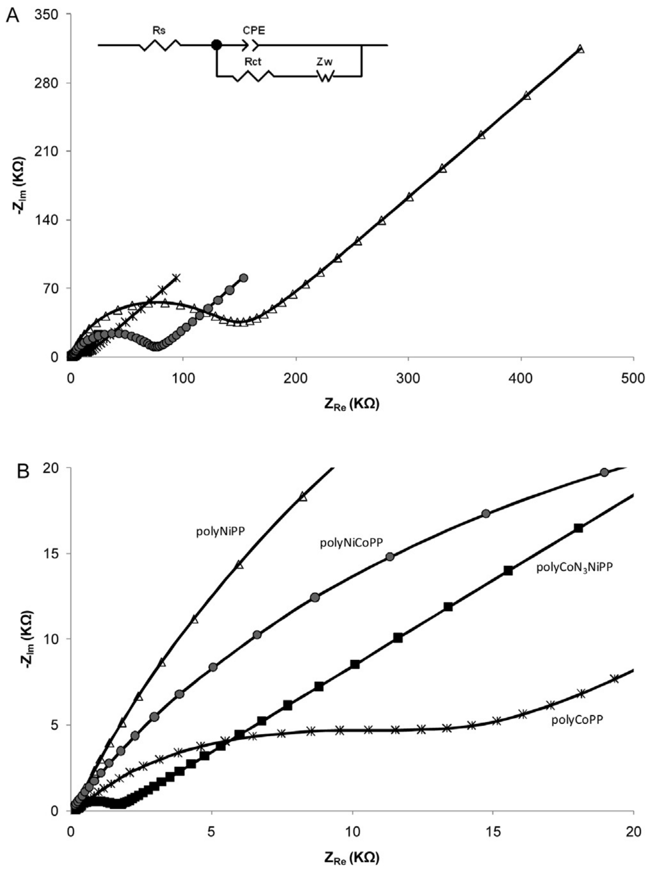

Fig. 6. Nyquist plots of different modified electrodes for 5 mM $Fe(CN)_6{}^{3-/4-}$ in 0.1 M KCl solution: (Δ) polyNiPP; (*) polyCoPP; (●) polyNiCoPP; (■) polyCoN$_3$NiPP; (−) fitted data. Inset shows the equivalent circuit representation. (B) is the enlarged EIS spectra.The working potential was set to +0.250 V (vs Ag/AgCl).

(with or without coordinated azide anion) were measured vs. the standard benchmark system $Fe(CN)_6{}^{3-}/Fe(CN)_6{}^{4-}$.This rapid and reversible outer sphere reaction allows evaluation of the electron transfer through the films [20]. Fig. 5 shows CV experiments as initial insights into the electron transfer processes at the different modified electrodes. The CV response of $Fe(CN)_6{}^{3-/4-}$ redox probe in 0.1 M KCl is only reversible for the polyCoN$_3$NiPP electrode (Fig. 5b), showing the highest peak current.

The Nyquist plots of the glassy carbon electrode modified with polyCoN$_3$NiPP were compared with the rest of the modifying phases, using $Fe(CN)_6{}^{3-}/Fe(CN)_6{}^{4-}$ as redox probe (Fig. 6). This experimental design can be described regarding a simple electrical equivalent circuit as illustrated in the inset of Fig. 6. The R_s is the solution/electrolyte resistance, R_{ct} is the charge transfer resistance, CPE is a constant phase element which replaces the double layer capacitance in the cases of inhomogeneous surfaces and Z_D is the diffusional impedance (Warburg) [21].

The apparent electron transfer rate constant (K_{app}) of $Fe(CN)_6{}^{3-}/Fe(CN)_6{}^{4-}$ for the different modified surfaces was calculated with Eq. (1). This equation is usually used to evaluate the high-frequency part of EIS spectra [22].

$$K_{app} = \frac{RT}{n^2F^2AR_{ct}C} \qquad (1)$$

A is the electrode area. The number of electrons involved in the oxidation/reduction of $Fe(CN)_6{}^{3-}/Fe(CN)_6{}^{4-}$ is n. R is the ideal gas constant; T is the temperature in Kelvin degree; F is Faraday constant, C is the concentration of $Fe(CN)_6{}^{3-}$ in mol cm^{-3}. Table 1 summarizes the obtained parameters for the equivalent circuit model and the resulting values for K_{app}.

The polyCoN$_3$NiPP architecture shows the highest K_{app} value, which is in agreement with the larger and resolvable peak separations observed in the Cyclic Voltammetry. This probably occurs because of the greater thermodynamic stability of the mixed-valence state which facilitates the charge transfer.

3.3. Detection of Sulfite anion

The electrode modified with polyCoN$_3$NiPP shows a shift of 400 mV to lower potentials for the oxidation Ep of the sulfite anion (700 mV), whereas the other systems do not change (Fig. S1 in supplementary information). Eq. (2) can explain this behavior, where the polyCoN$_3$NiPP mixed-valence complex catalyzes the sulfite oxidation.

$$At\,700\,mV : 2[polyCoN_3NiPP]^{3+} + SO_3^{2-} + H_2O \leftrightarrow 2[polyCoN_3NiPP]^{2+}$$
$$+HSO_4^- + H^+ 2[polyCoN_3NiPP]^{2+} \leftrightarrow 2[polyCoN_3NiPP]^{3+} + 2e^- \qquad (2)$$

The EIS experiments for the polyCoN$_3$NiPP are depicted in Fig. 7; the inset corresponds to the equivalent circuit proposed for the modified electrode. The graphic of $1/R_{ct}$ vs sulfite concentration (Fig. 8) shows a linear response from 0.1 to 3.4 mM, with a significant increase of sensitivity in more than ten times with respect to the bare electrode, y = 0.2620 KΩ^{-1} mM^{-1} x + 0.1653 KΩ^{-1} vs y = 0.0157 KΩ^{-1} mM^{-1} x + 0.0036 KΩ^{-1}.

There was a significant linear correlation between R_{ct} and sulfite concentration of wine samples at 700 mV (Table 2).

Table 3 compares other electrochemical systems for analysis of sulfite anion. As far as we know, polyCoN$_3$NiPP is the first impedimetric method described to measure sulfite anion.

Table 1
Comparative estimated electrochemical impedance parameters for different modified electrodes and K_{app} values calculated with Eq. (1) for $Fe(CN)_6{}^{3-}/Fe(CN)_6{}^{4-}$ (5 mM).

	Rs (Ω)	Rct (Ω)	Zw (Ω.s$^{-1/2}$)	CPE (μF)	*n*	K_{app} (cm s^{-1})
polyCoN$_3$NiPP	150.6 (10%)	1462.1 (6%)	18150 (5%)	0.067 (9%)	0.78 (0.8%)	58.5×10^{-6}
polyCoPP/azide	203.2 (10%)	14444 (6%)	64519 (6%)	0.27 (5%)	0.65 (0.6%)	1.17×10^{-6}
polyNiCoPP/azide	177.9 (10%)	72844 (4%)	63964 (9%)	0.029 (3%)	0.73 (0.6%)	0.71×10^{-6}
polyNiPP/azide	147.3 (11%)	120540 (7%)	247520 (10%)	0.012 (5%)	0.83 (0.5%)	0.59×10^{-6}
polyCoNiPP[a]	157.2 (9%)	116740 (2%)	137220 (8%)	0.022 (6%)	0.77 (0.2%)	0.73×10^{-6}
polyCoPP[a]	158.3 (10%)	30750 (5%)	130000 (6%)	0.067 (8%)	0.67 (0.7%)	0.55×10^{-6}
polyNiCoPP[a]	165.3 (11%)	95360 (5%)	124590 (10%)	0.065 (5%)	0.65 (0.5%)	0.54×10^{-6}
polyNiPP[a]	139.5 (8%)	103550 (4%)	168700 (6%)	0.077 (7%)	0.70 (0.8%)	0.69×10^{-6}

The values in brackets for *Rs*, *Rct*, *Zw*, CPE and *n* are the estimated error in percent (n = 3). The working potential was set to +0.250 V (vs Ag/AgCl).
[a] The polyporphyrinic modified glassy carbon electrodes are not in contact with azide.

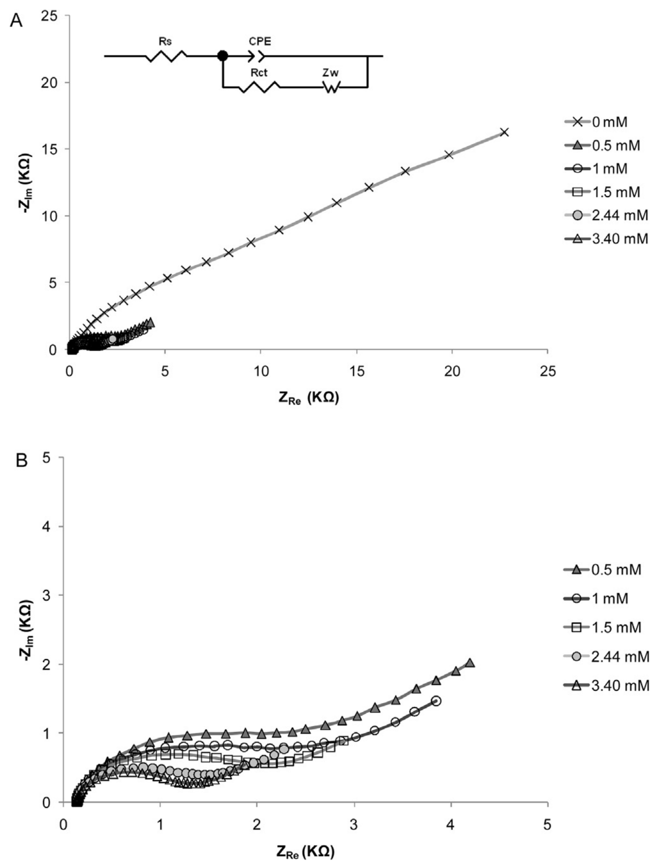

Fig. 7. Nyquist plots for polyCoN$_3$NiPP/GCE in 0.05 M KH_2PO_4/K_2HPO_4 buffer solution (pH 7.0) for 0-3.40 mM sulfite concentration range. Inset shows the equivalent circuit representation. (B) is the enlarged EIS spectra. The working potential was set to +0.700 V (vs Ag/AgCl).

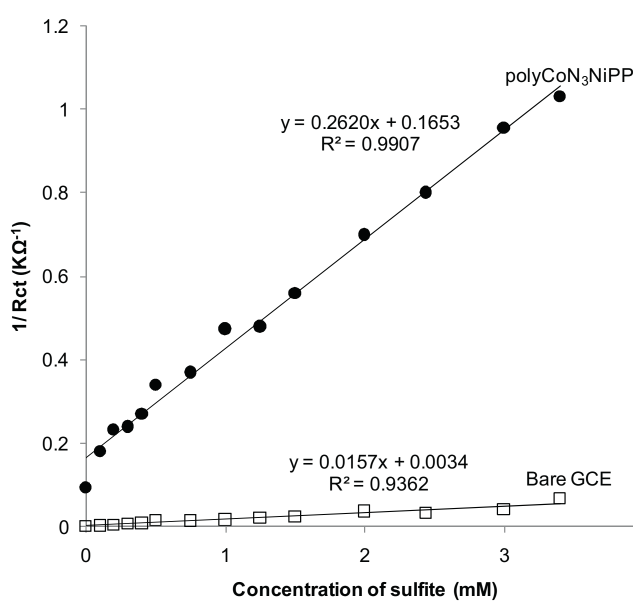

Fig. 8. 1/R_{ct} vs sulfite concentration calibration curves of (●) polyCoN$_3$NiPP/GCE and (□) bare GCE obtained in 0.05 M KH_2PO_4/K_2HPO_4 buffer solution (pH 7.0).

Table 2
Determination of sulfite in white wine samples using polyCoN$_3$NiPP/GCE and impedance measurements.

	SO_3^{2-} added/mM	Δ R_{ct}[a]/ohms	SO_3^{2-} found/mM
White wine sample free from sulfite	0.2	7250.5 ± 43	0.21 ± 0.01
	0.5	4099.4 ± 50	0.62 ± 0.01
	1	2608.5 ± 46	1.17 ± 0.03
	2	1629.9 ± 25	2.08 ± 0.04

[a] ΔR_{ct} corresponds to (R_{ct} for white wine sample free from sulfite – R_{ct} for same sample with sulfite added); *n* = 3.

Table 3
Comparison of the polyCoN$_3$NiPP/GCE with different sulfite detection systems.

Electrode	Potential (V)	Linear range (M)	Electrochemical Method	Determination in real sample	Ref.
Poly[(Ni-(protoporphyrin IX)]/GCE	+0.500 (vs Ag/AgCl)	1.4×10^{-5} to 2.7×10^{-4}	FIA-amperometry	No	[23]
Boron-Doped Diamond Electrode	+0.950 (vs Ag/AgCl)	2.5×10^{-6} to 2.5×10^{-4}	Amperometry	Yes	[24]
CuCoHCFCPE[a]	+0.720 (vs Ag/AgCl)	5×10^{-6} to 5×10^{-3}	CV	Yes	[25]
($[Mn_2^{IV} O_2(phen)_2(H_2O)_2]^{3+}$)/Nafion/GCE	+0.150 (vs SCE)	4.99×10^{-7} to 2.49×10^{-6}	CV without oxygen	No	[26]
PrHCF/GCE[b]	+0.650 (vs Ag/AgCl)	6×10^{-4} to 8×10^{-3}	LSV	Yes[c]	[27]
MWCNT/CPEs[d]	−0.500 (vs Ag/AgCl)	2.5×10^{-5} to 5×10^{-4}	SWV without oxygen	Yes	[28]
Graphene/carbon electrode	+0.900 (vs Ag/AgCl)	5×10^{-6} to 1.6×10^{-4}	FIA-amperometry	No	[29]
Carbon black paste Electrode	+0.650 V (vs SCE)	8×10^{-6} to 1×10^{-3}	SWV	Yes	[30]
polyCoN$_3$NiPP/GCE	+0.700 (vs Ag/AgCl)	1×10^{-4} to 3.4×10^{-3}	Impedimetric	Yes	[this work]

[a] Copper-Cobalt hexacyanoferrate carbon paste electrode.
[b] Praseodymium hexacyanoferrate (PrHCF)/glassy carbon electrode.
[c] But date not shown.
[d] Multiwalled carbon nanotubes/carbon paste electrode.

4. Conclusions

A very promising electroactive material that can be used for different analytical applications is described in this paper. The azide linked bimetallic structure behaves as a conductive phase exclusively when the polyCoPP is immobilized in the first place. This result is consistent with the formation of an organized structure ruled by a peroxo intermediate. As far as we know this is the first report of EIS detection of sulfite anion. The modified phase produces an increase of sensitivity to more than ten times for sulfite detection.

Acknowledgements

Financial support from University of Buenos Aires (UBACyT 2014-0469), ANPCyT (PICT 2013-1541) and CONICET (PIP 100029) are gratefully thanked.

Appendix A. Supplementary data

Supplementary data associated with this article can be found, in the online version, at http://dx.doi.org/10.1016/j.electacta.2016.11.161.

References

[1] S. Banerjee, A. Tyagi (Eds.), Functional Materials: Preparation Processing and Applications, 2011.
[2] S. Kubatkin, A. Danilov, M. Hjort, J. Cornil, J.L. Bredas, N. Stuhr-Hansen, P. Hedegard, T. Bjornholm, Single-electron transistor of a single organic molecule with access to several redox states, Nature 425 (2003) 698–701, doi:http://dx.doi.org/10.1038/nature02010.
[3] D.B. Brown, J.T. Wroblewski, in: D.B. Brown (Ed.), Mixed-Valence Compounds, Reidel Dordrecht, 1980, pp. 49.
[4] M.B. Robin, P. Day, Mixed Valence Chemistry, Advances in Inorganic Chemistry and Radiochemistry 10 (1967) 247–422, doi:http://dx.doi.org/10.1016/S0065-2792(08)60179-X.
[5] S. Santi, A. Bisello, R. Cardena, A. Donolib, Key multi(ferrocenyl) complexes in the interplay between electronic coupling and electrostatic interaction, Dalton Trans. 44 (2015) 5234–5257, doi:http://dx.doi.org/10.1039/C4DT03581J.
[6] M. Hamer, R. Carballo, I. Rezzano, Electrocatalytic Reduction of Hydrogen Peroxide by Nanostructured Bimetallic Films of Metalloporphyrins, Electroanalysis 21 (2009) 2133–2138, doi:http://dx.doi.org/10.1002/elan.200904645.
[7] M. Vago, V. Campodall'Orto, I. Rezzano, E.S. Forzani, E.J. Calvo, Metalloporphyrin electropolymerization: electrochemical quartz crystal microgravimetric studies, Journal of Electroanalytical Chemistry 566 (2004) 177–185, doi:http://dx.doi.org/10.1016/j.jelechem.2003.11.024.
[8] R.R. Carballo, V. Campodall'Orto, I.N. Rezzano, Supported bimetallic polymers of porphyrins as new heterogeneous catalyst, Journal of Molecular Catalysis A 280 (2008) 156–163, doi:http://dx.doi.org/10.1016/j.molcata.2007.10.035.
[9] J.P. Collman, R. Boulatov, Heterodinuclear Transition-Metal Complexes with Multiple Metal-Metal Bonds, Angew. Chem. Int. Ed. 41 (2001) (2002) 3948–3961, doi:http://dx.doi.org/10.1002/1521-3773(1104)41:21<3948::AID-ANIE3948>3.0.CO;2-K.
[10] K. Hüttinger, C. Förster, K. Heinze, Intramolecular electron transfer between molybdenum and iron mimicking bacterial sulphite dehydrogenase, Chem. Comm. 50 (2014) 4285–4288, doi:http://dx.doi.org/10.1039/C3CC46919K.
[11] S. Robin, M. Arese, E. Forte, P. Sarti, O. Kolaj-Robin, A. Giuffrè, T. Soulimane, Functional Dissection of the Multi-Domain Di-Heme Cytochrome c550 from Thermus thermophilus, PLoS One 8 (2013) e55129, doi:http://dx.doi.org/10.1371/journal.pone.0055129.
[12] S.R. Batten, S.M. Neville, D.R. Turner, Coordination Polymers: Design, Analysis and Application, Royal Society of Chemistry, Cambridge, 2009.
[13] J. Ribasa, A. Escuera, M. Monforta, R. Vicente, R. Cortés, L. Lezama, T. Rojo, Polynuclear Ni^{II} and Mn^{II} azido bridging complexes. Structural trends and magnetic behavior, Coordination Chemistry Reviews 193–195 (1999) 1027–1068, doi:http://dx.doi.org/10.1016/S0010-8545(99)00051-X.
[14] T. Yao, J. Lu, D. Li, J. Dou, A mixed-valence complex of cobalt based on 3-methoxysalicylaldoxime, Acta Cryst. C 70 (2014) 364–367, doi:http://dx.doi.org/10.1107/S2053229614005245.
[15] D.A. Adler, F.R. Longo, F. Kampas, J. Kim, On the preparation of metalloporphyrins, J. Inorg. Nucl. Chem. 32 (1970) 2443–2445.
[16] K.A. Macor, T.G. Spiro, Porphyrin electrode films prepared by electrooxidation of metalloprotoporphyrins, J. Am. Chem. Soc. 105 (1983) 5601–5607, doi:http://dx.doi.org/10.1021/ja00355a012.

[17] J.P. Collman, A. Dey, R.A. Decréau, Y. Yang, Model Studies of Azide Binding to Functional Analogues of CcO, Inorg. Chem. 47 (8) (2008) 2916–2918, doi: http://dx.doi.org/10.1021/ic702294n.
[18] M. Layek, M. Ghosh, S. Sai, M. Fleck, P.T. Muthiah, S.J. Jenniefer, J. Ribas, D. Bandyopadhyay, Synthesis, crystal structure and magnetic properties of nickel (II) and cobalt(III) complexes of a pentadentate Schiff base, Journal Molecular Structure 1036 (2013) 422–426, doi:http://dx.doi.org/10.1016/j.molstruc.2012.11.068.
[19] V.A. Adamian, F. D'souza, S. Licoccia, M.L. Di Vona, E. Tassoni, R. Paolesse, T. Boschi, K.M. Kadish, Synthesis, Characterization, and Electrochemical Behavior of (5,10,15-Tri-X-phenyl-2,3,7,8,12,13,17,18-octamethylcorrolato)cobalt(III) Triphenylphosphine Complexes, Where X = p-OCH_3, p-CH_3, p-Cl, m-Cl, o-Cl, m-F, o-F, or H, Inorg. Chem. 34 (1995) 532–540, doi:http://dx.doi.org/10.1021/ic00107a003.
[20] N. Oyama, T. Ohsaka, M. Kaneko, K. Sato, H. Matsuda, Electrode kinetics of the $Fe(CN)_6^{4-/3-}$ and $Fe(CN)_5^{3-/2-}$ complexes confined to polymer film on graphite surfaces, J. Am. Chem. Soc. 105 (1983) 6003–6008.
[21] X.-Z. Yuan, C. Song, H. Wang, J. Zhang, Electrochemical Impedance Spectroscopy in PEM Fuel Cells, Springer, 2010, doi:http://dx.doi.org/10.1007/978-1-84882-846-9.
[22] D. Nkosi, K.I. Ozoemena, Self-assembled nano-arrays of single-walled carbon nanotube-octa(hydroxyethylthio)phthalocyaninatoiron(II) on gold surfaces: Impacts of SWCNT and solution pH on electron transfer kinetics, Electrochimica Acta 53 (2008) 2782–2793, doi:http://dx.doi.org/10.1016/j.electacta.2007.10.073.
[23] R. Carballo, V. Campodall'Orto, A.L. Balbo, I. Rezzano, Determination of sulfite by flow injection analysis using a poly[Ni-(protoporphyrin IX)] chemically modified electrode, Sensors and Actuators B 88 (2003) 155–161, doi:http://dx.doi.org/10.1016/S0925-4005(02)00319-2.
[24] C. Chinvongamorn, K. Pinwattana, N. Praphairaksit, T. Imato, O. Chailapakul, Amperometric Determination of Sulfite by Gas Diffusion- Sequential Injection with Boron-Doped Diamond Electrode, Sensors 8 (2008) 1846–1857, doi: http://dx.doi.org/10.3390/s8031846.
[25] A. Siroueinejad, A. Abbaspour, M. Shamsipurb, Electrocatalytic Oxidation and Determination of Sulfite with a Novel Copper-Cobalt Hexacyanoferrate Modified Carbon Paste Electrode, Electroanalysis 21 (12) (2009) 1387–1393, doi:http://dx.doi.org/10.1002/elan.200804535.
[26] Machini W.B.S, M.F.S. Teixeira, Electrochemical Properties of the Oxo-Manganese-Phenanthroline Complex Immobilized on Ion-Exchange Polymeric Film and Its Application as Biomimetic Sensor for Sulfite Ions, Electroanalysis 26 (2014) 2182–2190, doi:http://dx.doi.org/10.1002/elan.201400289.
[27] B. Devadas, M. Sivakumar, S.M. Chen, S. Cheemalapati, An electrochemical approach: Switching Structures of rare earth metal Praseodymium hexacyanoferrate and its application to sulfite sensor in Red Wine, Electrochimica Acta 176 (2015) 350–358, doi:http://dx.doi.org/10.1016/j.electacta.2015.07.022.
[28] E.M. Silva, R.M. Takeuchi, A.L. Santos, Carbon nanotubes for voltammetric determination of sulphite in some Beverages, Food Chemistry 173 (2015) 763–769, doi:http://dx.doi.org/10.1016/j.foodchem.2014.10.106.
[29] N. Zainudin, M.M. Yusoff, K.F. Chong, A promising electrochemical sensing platform based on a graphene nanomaterials for sensitive sulfite determination, 2nd International Conference on Biomedical Engineering (ICoBE), 30–31 March 2015, Penang, 2015, doi:http://dx.doi.org/10.1109/ICoBE.2015.7235886.
[30] L. Xu, F. Guo, Y. You, J. Hu, Y. Miao, Z. Wu, L. Wang, Simple Electrochemical Sensor Based on Carbon-black Paste Electrode Coupled with Derivative Square Wave Voltammetry for the Determination of Sulfites in Rice Wine, Int. J. Electrochem. Sci. 11 (2016) 4586–4597, doi:http://dx.doi.org/10.20964/2016.06.43.